International Journal of Geo-Information

MDPI

Case Report

Mapping Coastal Flood Susceptible Areas Using Shannon's Entropy Model: The Case of Muscat Governorate, Oman

Hanan Al-Hinai * and Rifaat Abdalla

Earth Sciences Department, College of Science, Sultan Qaboos University, Sultanate of Oman, P.O. Box 36, Al-Khoud P.C. 123, Oman; rabdalla@squ.edu.om

* Correspondence: s24410@student.squ.edu.om

Abstract: Floods are among the most common natural hazards around the world. Mapping and evaluating potential flood hazards are essential for flood risk management and mitigation strategies, particularly in coastal areas. Several factors play significant roles in flooding and recognizing the role of these flood-related factors may enhance flood disaster prediction and mitigation strategies. This study focuses on using Shannon's entropy model to predict the role of seven factors in causing floods in the Governorate of Muscat, Sultanate of Oman, and mapping coastal flood-prone areas. The seven selected factors (including ground elevation, slope degree, hydrologic soil group (HSG), land use, distance from the coast, distance from the wadi, and distance from the road) were initially prepared and categorized into classes based on their contribution to flood occurrence. In the next step, the entropy model was used to determine the weight and contribution of each factor in overall susceptibility. Finally, results from the previous two steps were combined using ArcGIS software to produce the final coastal flood susceptibility index map that was categorized into five susceptibility zones. The result indicated that land use and HSG are the most causative factors of flooding in the area, and about 133.5 km^2 of the extracted area is threatened by coastal floods. The outcomes of this study can provide decision-makers with essential information for identifying flood risks and enhancing adaptation and mitigation strategies. For future work, it is recommended to evaluate the reliability of the obtained result by comparing it with a real flooding event, such as flooding during cyclones Gonu and Phet.

Keywords: ArcGIS software; coastal flood susceptibility index; digital elevation model DEM; influencing factors; precondition factors; trigger factors; muscat governorate; sultanate of Oman; shannon's entropy model; wadi

Citation: Al-Hinai, H.; Abdalla, R. Mapping Coastal Flood Susceptible Areas Using Shannon's Entropy Model: The Case of Muscat Governorate, Oman. *ISPRS Int. J. Geo-Inf.* **2021**, *10*, 252. https://doi.org/10.3390/ijgi10040252

Academic Editors: Raffaele Albano and Wolfgang Kainz

Received: 12 February 2021
Accepted: 4 April 2021
Published: 9 April 2021

1. Introduction

The global effects of climate change and its related phenomena make coastal environments more vulnerable to natural hazards [1]. Coastal flooding is one of the world's contemporary issues, especially for human lives (loss of life and injury), properties and infrastructure [2]. Coastal flooding also threatens significant resources and environments along coastal regions. For instance, as per the statistical report published in [3], floods in 2019 accounted for 49% of the total number of natural disasters, about 33% of the total number of people affected, and about 43% of victims worldwide. In coastal areas, floods often happen when sea levels along the coast are above regular tide levels, resulting in inundations that may last for several days [4]. Tidal changes, storms, heavy rains, or overflowing streams are some of the sources that may cause flooding in coastal areas [5]. Even though flood prevention is almost impossible, successful flood management approaches can be taken in order to prevent or reduce the threats posed by these risks [6]. In general, four major phases (mitigation, preparedness, response, and recovery) are involved in managing any risk [7]. Flood susceptibility mapping is an essential step in flood risk management approaches, which can be defined as a quantitative or qualitative assessment

of flood spatial distribution that occurs or is likely to occur in an environment [8]. It is used to predict where floods are likely to occur, regardless of the temporal probability of flooding, such as when or how often the floods occur [9]. For instance, a study by El-Haddad et al. [10] applied four novel models named boosted regression tree (BRT), functional data analysis (FDA), general linear model (GLM), and multivariate discriminant analysis (MDA) to perform flood susceptibility mapping in the Wadi Qena Basin, Egypt. The study indicated that the created maps could be adopted by the local government and decision-makers to implement appropriate mitigation plans for future flood damages. Another study by Samanta et al. [2] evaluated the flood susceptibility of the middle and lower parts of Subarnarekha Basin (India), using ground observations and frequency ratio technique to perform appropriate flood management and future planning strategies. Hence, identifying the most vulnerable areas to flooding helps decision-makers to develop appropriate mitigation and preparedness strategies before and after disasters.

There are several factors that play significant roles in flooding. Predicting flood-prone coastal areas requires consideration of all factors that affect them. These factors, also known as causative factors [8,11,12], conditioning factors [2,6,13], influencing factors [14,15], or influencing indicators [16], are needed as an independent factor contributing to flood incidence in a particular area [17], and can have a major impact on the accuracy of the maps produced [12]. They also reflect the physical characteristics of the area being investigated, and each causes flood differently and cumulatively [13]. Low-lying areas, for instance, are more susceptible to flooding than others, as water is more likely to flow from high to low areas. Steep slopes, on the other hand, tend to slow infiltration and increase surface runoff, which leads to increased flood risk [14,18]. Besides, changes in land-use patterns that form an impermeable surface can increase the velocity of the flow and thus contribute to flooding in the area [19]. Accordingly, the factors of lower elevations and steep slopes as well as impermeable surfaces tend to increase the susceptibility to flooding in a particular area. Flood influencing factors are categorized into precondition and trigger factors based on their hazards forming contribution. Factors of the precondition are constant or change very little over a long period. With regard to coastal floods, flat and low-lying ground, low surface infiltration capacity, and coastal buffer zone, are some examples of precondition factors. Trigger factors are constantly changing as compared with precondition factors. The key trigger factors causing coastal floods are heavy rains, tropical cyclones induced storm surges, tidal waves, and tsunamis [20,21].

So far, a variety of regional and international studies have been suggested by researchers using different models and techniques for accurate mapping and assessing of potential flood-prone regions. Such models and techniques can be used to map different scales of areas, including global, regional, or national scales, with the use of different flood influencing factors [8,22]. One of the most popular models is Shannon's entropy model [23] which has been extensively used in hazard and risk assessment studies to calculate the weight index of natural hazards. Additional entropy in the index system is provided by several important factors. Hence the entropy value can be used to measure the index system's objective weights [24]. In flood hazard research, entropy is used to assess the role of factors in triggering a hazard by measuring the information contained in certain factors, where higher weight factors contribute more to flood hazard than lower weight factors [25]. For instance, the analysis [20] measured the susceptibility of each county in the Yangtze River Delta of China to various hazards using the entropy-weight model. Another analysis [26] successfully recognized flood-prone areas in Madarsoo watershed in Iran using the entropy model. In the same region, the author [27] investigated the use of frequency ratio and entropy models for flood susceptibility mapping. Another research [28] compared the results of applying frequency ratio model and entropy model to predict flood susceptibility in the repeatedly and severely flood-affected area of Middle Ganga Plain.

In a previous study conducted by Al-Hinai and Abdalla [16] for the Governorate of Muscat, the entropy model was used within the geographic information system (GIS) environment to analyze four influencing indicators to predict their role in causing flooding,

and to map areas exposed to coastal flooding. This study aims to include further factors as they play critical roles in water infiltration and runoff behaviors. It is noteworthy to remark that the analysis focused only on the precondition factors, referred to here as influencing factors, while the triggering factors were not addressed. This paper is structured as follows: Section 2 briefly describes the study area, Section 3 describes in detail the materials and method used for mapping coastal flood susceptible areas, Section 4 explains and addresses the main finding of the study, and finally the concluding remarks are reported in Section 5.

2. Study Area

Muscat Governorate (Figure 1), Sultanate of Oman's capital, is located in the north-eastern part of the country where the Tropic of Cancer passes a few kilometers south of the governorate [29]. The Governorate covers an area of 3500 km^2, and overlooks the Sea of Oman with a coastline of 200 km long [30]. Administratively, Muscat Governorate consists of six wilayats (regions), of which only five overlook the Sea of Oman, including Seeb, Bawshar, Mutrah, Muscat and Qurayyat [31]. Hence, this study refers only to these wilayats. The total population of Muscat Governorate in 2020 was about 1,302,440 people [32]. Coastal areas exhibit greater population growth rates and urbanization than other regions [33].

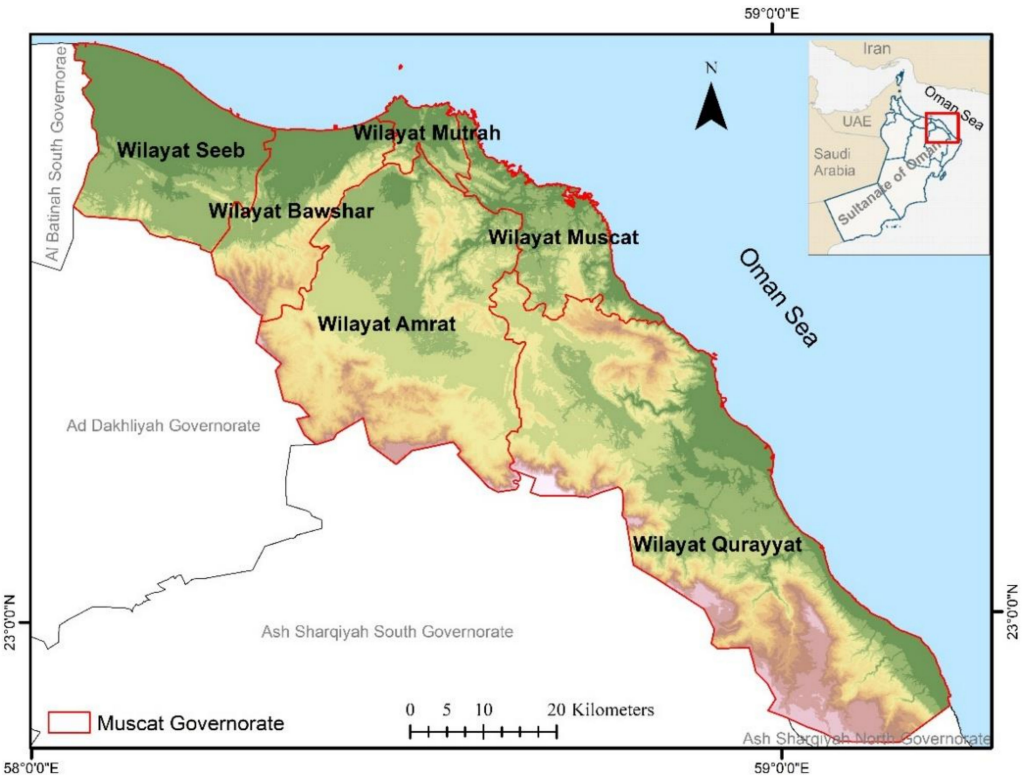

Figure 1. The location map of Muscat Governorate and its wilayats.

The climate of the country is generally hot and dry, as is the case in other parts of the Arabian Peninsula [34]. The annual temperatures reach over 45 °C in summer and drop to 15 °C in winter. Annual precipitation is relatively low in most part of the country, reaching less than 100 mm [29]. The governorate is surrounded by mountains with high topographic elevation (−0.3–1967 m), slope (0–89 degrees), rough surface soil, and dry conditions [35]. There are a significant number of wadies (valleys) that extend throughout the governorate, descending from the mountains and flowing into the Sea of Oman [35,36]. Such wadies lead to several floods, including flash floods and coastal flooding, which have been reported in Oman [36,37].

The Sultanate has become more vulnerable to extreme weather events, cyclones and tsunamis due to its location overlooking the Arabian tectonic plate and the Indian Ocean, where tsunami and tropical storms occur [38]. For instance, the Sultanate of Oman in general and Muscat Governorate in particular were affected by two powerful tropical cyclones; Gonu in 2007, and Phet in June 2010 [39]. In addition, Oman's coastline has been hit by the tsunami several times, the best known of which was the 1945 Makran tsunami [40], and the 2004 Indian Ocean tsunami [41].

Given this situation, it is crucial to analyze and map the coastal flood-prone potential areas in the Governorate of Muscat to introduce proactive steps that can mitigate flood losses.

3. Data Used and Methodology

Several steps have been taken to identify and map potential coastal flooding areas within the Governorate of Muscat. The first step involved selecting, preparing, and classifying the influencing factors using the ArcGIS 10.4 software. Accordingly, the entropy model was used in the second step to specify the weight and contribution of each factor in overall susceptibility using Microsoft Excel software. Finally, the results from the previous two steps were integrated in the third step using ArcGIS 10.4 software to produce the final coastal flood susceptibility map. The methodology adopted for this study is illustrated in Figure 2.

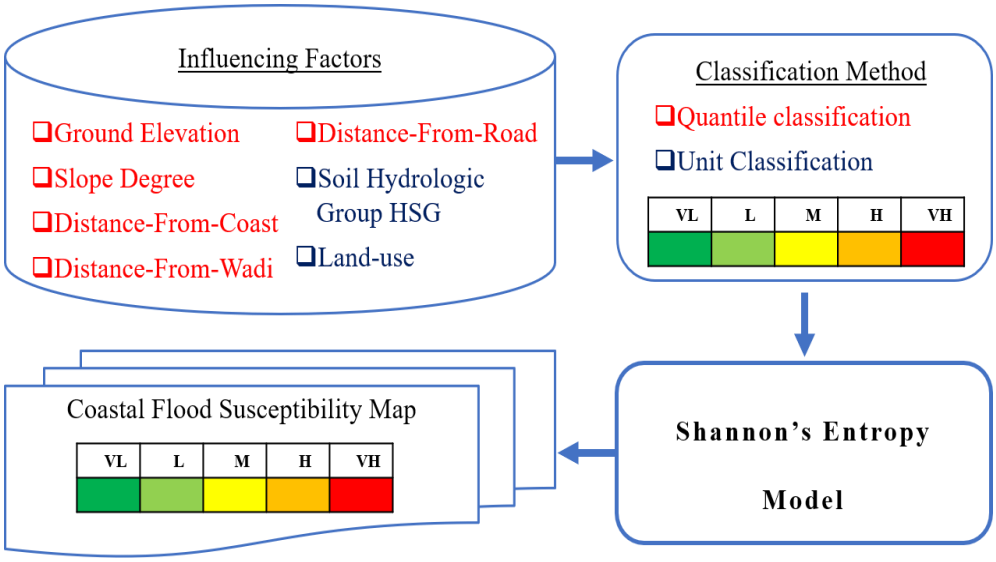

Figure 2. The methodology adopted for this study: (VL) is very low, (L) is low, (M) is moderate, (H) is high, and (VH) is very high.

3.1. Coastal Flood Influencing Factors

Selecting the influencing factors is the most significant stage in producing the final maps of coastal flood susceptibility. Even though there is no clear guidance in specifying flood influencing factors, several literatures have used certain factors indicating their critical role in flood susceptibility mapping [42]. Therefore, this study used seven influencing factors for the modelling aims. These are ground elevation, slope angle, hydrologic soil group (HSG), land use, distance from coast, distance from wadi (stream), and distance from road.

Ground elevation, as it regulates the direction of flow movement (due to the Earth's gravity, waters always move from higher to lower elevations) as well as the depth and extent of flooding [43], is one of the most significant factors commonly used in flood studies. Elevation and flood are inversely related; flood increases with decreasing elevation and hence areas of low elevation are more vulnerable to flooding [44]. Slope angle (in degrees) is another important flooding factor as it directly affects surface runoff and infiltration.

As the gradient rises, the surface runoff rises significantly; consequently, infiltration time decreases, leading to flooding [45]. The HSG factor has been widely recognized as a major factor affecting runoff processes, where soil diversity controls the surface runoff and the amount of water that can penetrate into the ground. In other words, as the ability of soil to infiltrate decreases, the risk of flooding increases [2]. The Natural Resource Conservation Service has categorized soils into four hydrological groups; A, B, C and D. Group A soils have the highest infiltration rates and the lowest potential runoff, and group D soils have the lowest infiltration rates and greatest potential of runoff [46]. Different types of land use have different penetration capabilities, evapotranspiration, and runoff coefficients [47]. Cultivated areas, for instance, provide levels of protection mechanisms that make the land less vulnerable to flooding, whereas urban areas increase the water runoff due to their largely impermeable surfaces, which makes the land more vulnerable to flooding [48]. Hence, the land-use factor may also make a major contribution to flooding. Factors distance-from-wadi and distance-from-coast play an important role in determining the flood zone. Regions close to the coast or wadi are more prone to flooding than regions further away [15]. The same condition applies to the distance from road, as roads and surrounding areas provide sealing surfaces that minimize infiltration potential and are a source of runoff with a substantial impact on flood rates [49].

In this study, it is worth mentioning that it was assumed that the maximum potential coastal flood limit would not exceed 2 km from the coast. Based on this assumption, areas between the coast and 2 km inland were only included in this study. In ArcGIS 10.4 software environments, maps of ground elevation and slope were created by analyzing a digital elevation model (DEM) with a spatial resolution of 5 m. The DEM raster data were obtained from Oman National Spatial Data Infrastructure (NSDI) portal [50], that were generated from aerial photos (at size of 50 cm pixel). The vector layers of the wadi channel obtained from the Ministry of Agriculture, Fisheries and Water Resources database, and the road network obtained from NSDI portal [50] were used to produce the distance from wadi and distance from road maps, using the Euclidean tool. A coastline layer acquired from NSDI portal [50] and a multiple ring buffer tool were used to prepare five distance-from-coast classes, as specified in Table 1. The local land-use layer obtained from the Ministry of Housing was classified into five categories based on their contribution to flooding as explained earlier in this section. The local soil detail layer obtained from the Ministry of Agriculture, Fisheries and Water Resources database was used to define the HSG as suggested in [36,37]. Only three groups of HSG were observed in the study area (group A, B, and C).

To convert the pattern of maps into measurable and comparable classes, several classification approaches have been used widely. Each approach is ideal for a specific application depending on the complexity of the data and the study objective [51]. ArcGIS Software contains several approaches to reclassify susceptibility maps such approaches are, “equal intervals”, “natural breaks”, “standard deviation”, “Manual Interval”, and “Quantile”. For instance, equal intervals are used to split the range of attribute values into classes of equal size [52], and this approach is accurate when a normal distribution of the data is present [53]. Classes in natural breaks jenks method are based on natural groupings inherent in the data where class breaks are defined to group common values and reduce class differences [52]. This approach is proper when there is a sudden and big jump in the dataset [53], and it is commonly used to classify continuous data [28]. In standard deviation, features are classified based on how much their values differ from the mean. Manual interval is used to manually define and set class ranges that are appropriate for the data [52]. In the quantile classification method, each class has an equal number of features, and groups pixels into classes of the same size. This approach is useful for minimizing the impact of the classification algorithm on results [6,42]. In this study, the ground elevation, slope angle, distance from wadi and distance from road factors were classified using the quantile classification method into five classes: very high, high, moderate, low and very low. For the further processing necessities of this study, land use and HSG layers were converted

from vector to raster format with the same cell size of 5 m as the DEM resolution. Table 1 summarizes the selected factors involved in mapping coastal flood susceptibility, their classes and their contribution rates, where 5 represent very high contribution and 1 very low contribution. Figure 3a–g displays the spatial distribution of the seven influencing factors along the coast of the Governorate of Muscat.

Table 1. The selected factors involved in mapping coastal flood susceptibility, their classes and their ratings.

Factor	Classes	Area km^2	Rating
Ground Elevation (m)	−0.283–3.41	41.51	5—very high
	3.42–18.2	141.34	4—high
	18.3–55.2	69.81	3—moderate
	55.3–122	62.72	2—low
	123–943	59.13	1—very low
Slope Angle (degree)	0–0.99	63.18	5—very high
	1–2.6	91.28	4—high
	2.7–8.2	79.41	3—moderate
	8.3–28	70.35	2—low
	29–84	70.27	1—very low
HSG	Group C	221.2377	4—high
	Group B	59.2654	3—moderate
	Group A	76.4368	2—low
Land Use	Built-Up Area	120.7383	5—very high
	Others	3.2249	4—high
	Nature Reserve	2.1427	3—moderate
	Agriculture / Park	9.1791	2—low
	Dam	0.0004	1—very low
Distance from Coast (m)	<500	104.3	5—very high
	500–750	45.237	4—high
	750–1000	43.721	3—moderate
	1000–1500	85.279	2—low
	1500–2000	83.504	1—very low
Distance from Wadi (m)	0–117.6	50.16	5—very high
	117.7–305.9	53.33	4—high
	306–596.1	52.99	3—moderate
	596.2–1075	51.9	2—low
	1076–2000	51.65	1—very low
Distance from Road (m)	0–31.37	63.84	5—very high
	31.38–133.3	73.71	4—high
	133.4–345.1	69	3—moderate
	345.2–729.4	67	2—low
	729.5–2000	66.37	1—very low

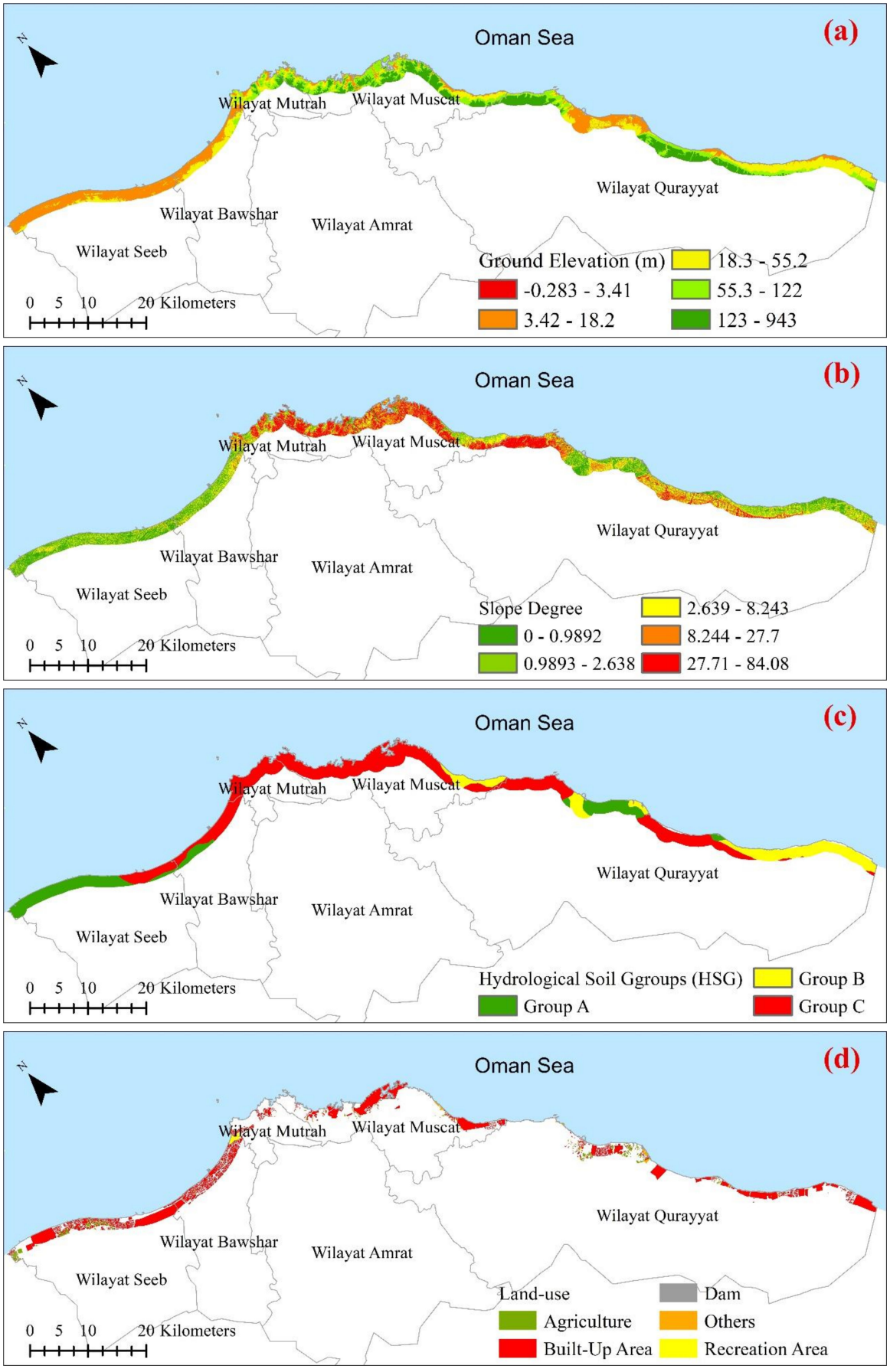

Figure 3. *Cont.*

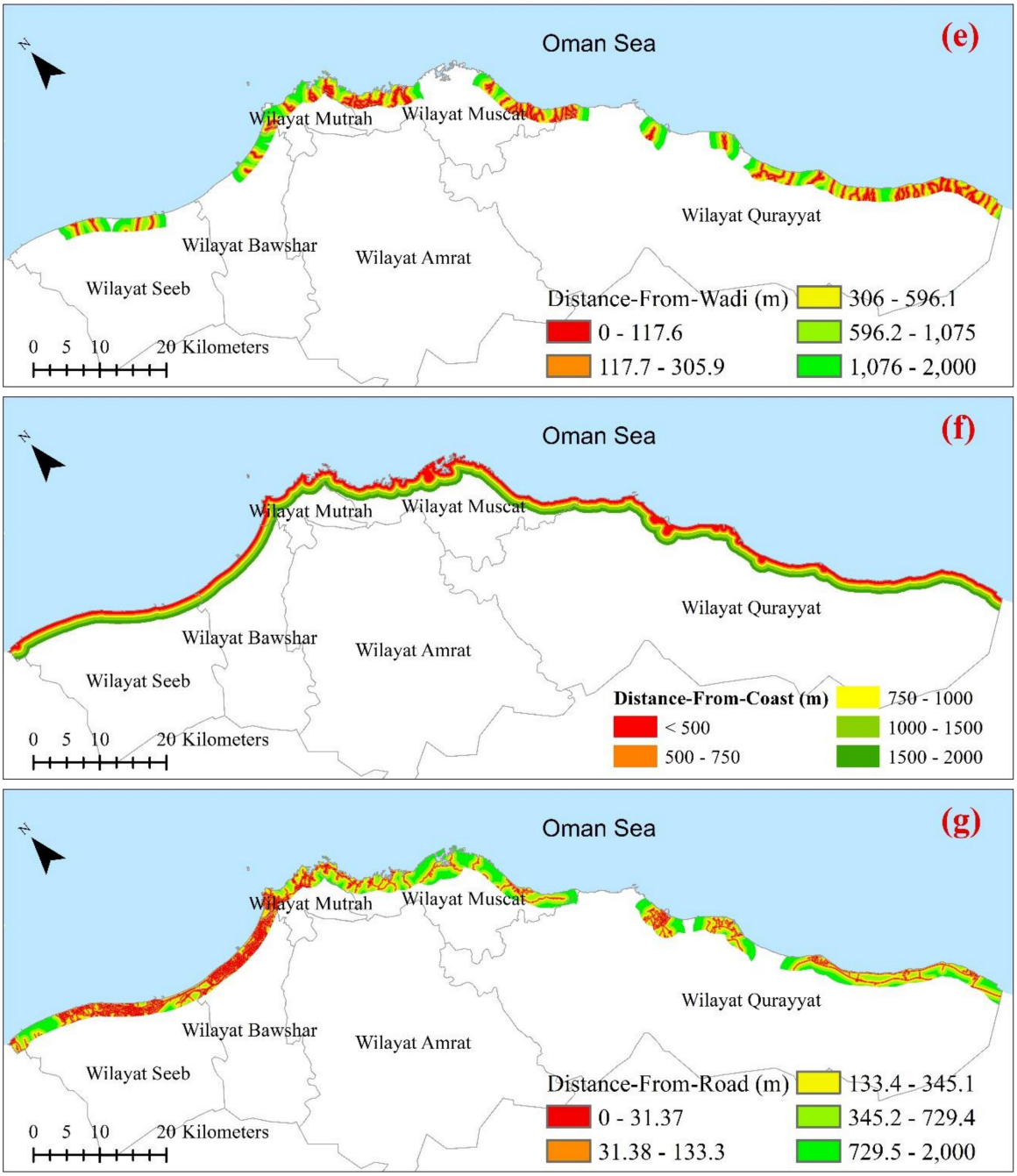

Figure 3. Spatial distribution of the influencing factors. (**a**) Ground elevation; (**b**) slope; (**c**) HSG; (**d**) land use; (**e**) distance-from wadi; (**f**) distance from coast; and (**g**) distance from road.

3.2. Entropy Model Implementation

The entropy model, which was initially introduced by Shannon [23], is a management approach that is used to eliminate the disorder, instability, and uncertainty in the system. In hazard and risk assessment studies, the entropy model has been extensively applied to determine the weighted index of natural hazards and to reflect the priority within certain factors in influencing a certain hazard [15,19–22]. For mapping flood susceptibility, the entropy model measures and reflects the contribution of influencing factors to flooding in the area, where higher weight factors contribute to flood hazard greater than low weight factors. Based on factors' weights, a final coastal flood susceptibility index map can be prepared. The calculation process of weight in this study is described as follows [16,20], with the help of Microsoft Excel and ArcGIS 10.4 Software.

First, assume x_j (j = 1, 2, 3, . . .) represents the different factors, and x_i (i = 1, 2, 3, . . .) represents the classes in these factors. Then the ith class attribute value in the jth factor is represented by x_{ij}, and the assessment method for the weight can be built on that basis. As the different dimensions between the different factors during the assessment are not identical, these factors should be standardized using Equation (1).

$$y_{ij} = \frac{x_{ij}}{\sum_{i=0}^{m} x_{ij}}, \ 0 \le y_{ij} \ \le 1 \tag{1}$$

where y_{ij} is the specific gravity value per x_{ij}, and m is the number of classes.

Second, calculate the entropy for each factor e_j using Equation (2).

$$e_j = \ -k \sum_{i=1}^{m} y_{ij} \ln y_{ij}, \ k = \ \frac{1}{\ln(m)} \tag{2}$$

where e_j is the entropy value, and k is a positive coefficient value determined by the sample size m (number of classes). $k = 1/\ln(m)$ is to ensure that $0 \le e_j \le 1$.

The degree of coefficient difference between the various factors h_j is calculated by following Equation (3), where the value of the smaller entropy coefficient e_j indicates a greater difference between the factors h_j. Hence, it indicates the effect of the factor is greater.

$$h_j = 1 - e_j \tag{3}$$

Third, calculate the weight w_j of each factor j using Equation (4).

$$wj = \frac{h_j}{\sum_{j=1}^{n} h_j} \tag{4}$$

where w_j is the weight of the j^{th} factors, and n is the number of conditioning factors in which the smaller the entropy value of factor, the greater weight in the comprehensive evaluation.

After determining the final weight for each factor, the coastal flood susceptibility index map was produced using the ArcGIS raster calculator tool and calculated using Equation (5).

$$FSI = \sum_{j=1}^{n} W_j \ Nor(\mathrm{F}_j) \tag{5}$$

where FSI is a degree of flood susceptibility index, W_j denotes the weight of each factor and $Nor(\mathrm{F}_j)$ is the normalized rate for each flood influencing factor to have a value between 0 and 1.

The resulting maps of Equation (5) were then reclassified into five susceptibility classes for mapping, validation, and discussion, which included very high, high, moderate, low, and very low. This classification was performed using the quantile classification method.

4. Results and Discussion

For predicting and mapping the susceptibility of the Governorate of Muscat to coastal floods, seven factors were evaluated and weighted according to Equation (4) with the use of ArcGIS 10.4 software and Microsoft Excel. The weights derived from this entropy model for each factor are summarized in Figure 4, wherein the higher the weight factor, the greater the flood probability contribution by that factor.

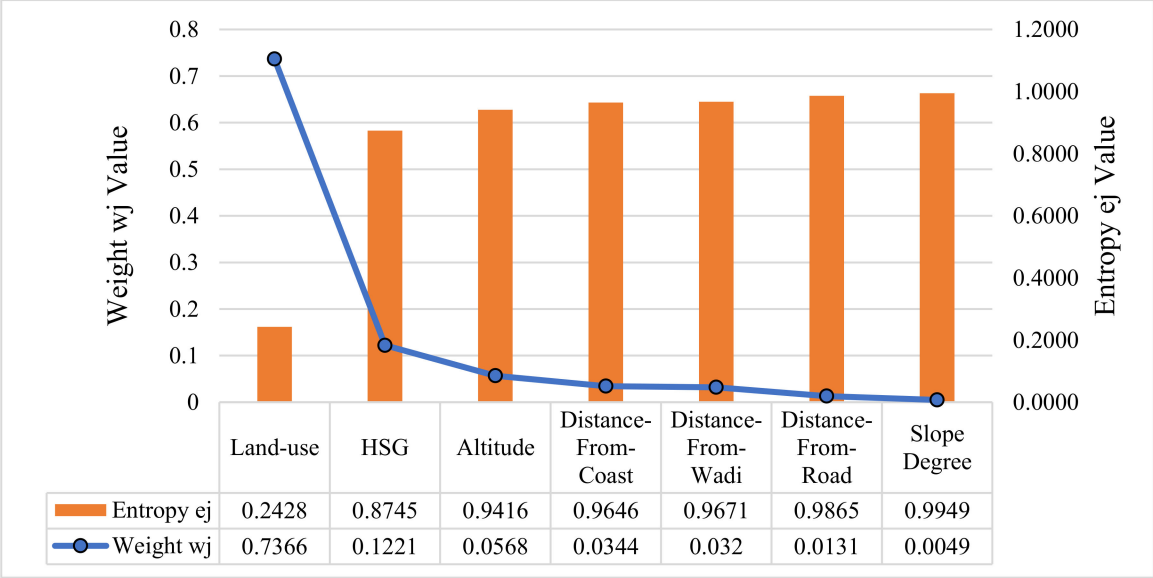

Figure 4. The entropy (e_j) and weight (w_j) factor values.

According to the values of the weighted factors, land use has the highest value (0.7366), followed by HSG (0.1221), ground elevation (0.0568), distance from coast (0.0344), distance from wadi (0.0320), and distance from road (0.0131), whereas the slope degree has the lowest weight value (0.0049). As a consequence, land use has the greatest contribution to flood risk, while slope degree has the lowest impact on coastal flooding in the region. These results are incompatible with previous research [16] conducted for the same region, which concludes that the HSG factor has the highest contribution to flood risk in Wilayats Bawshar, Mutrah, Muscat, and Qurayyat, while the elevation factor has the highest contribution in Wilayat Seeb. These differences are due to three reasons. The first is that this study analyzed seven factors (ground elevation, slope degree, HSG, land use, distance from coastline, distance from wadi, and distance from road), while four factors (ground elevation, slope degree, HSG, and distance from coastline) were analyzed in the previous study. This indicates that if the model's input factors change, the evaluation results will subsequently change. The second reason relates to the classification techniques applied within each factor to classify their contribution in influencing flood, as the input factor classification technique has major impacts on the flood hazard outcomes. The previous study classified factors based on published literatures [26,39,54]. While in this study, a quantile classification technique was applied for ground elevation, slope degree, distance from wadi, and distance from road factors, whereas land use and HSG factors used unit-based classification. The third reason relates to the extent of the study area, as the classification range between categories of each factor changes based on the size of the study area. The previous study analyzed the susceptibility to coastal flood for each Wilayat of the Governorate of Muscat individually, while in this study the Governorate of Muscat was analyzed as one zone. Furthermore, it is worth mentioning that most studies that used the entropy method to assess the relationship between flood occurrence and influencing factors indicated that there is no common factor contributing to flood risk more than other factors. For instance, the result of this study indicates that land use has the highest weight, which contributes more to the occurrence of floods. In comparison, the result of the study [26] showed that the maximum weight is allocated to the drainage density factor, while another study [54] concluded that lithology and curvature have the greatest contribution to the occurrence of flooding. This proves that the results of any study using the entropy method to analyze the relationship between flood occurrence and factors are based on the physical characteristics of the area under investigation and the number of factors used.

Once the weight of each factor was determined, the final degree of the coastal flood susceptibility index was calculated using Equation (5). It was found to range between

1.028 and 5.311, where higher values indicate a higher probability of coastal flooding. For mapping and discussion purposes, a quantile classification method was employed to classify the value into five susceptibility zones: very high, high, moderate, low, and very low as presented in Figure 5. In this figure, the red color reflects areas with very high flood potential, while the dark green color reflects areas with very low flood potential.

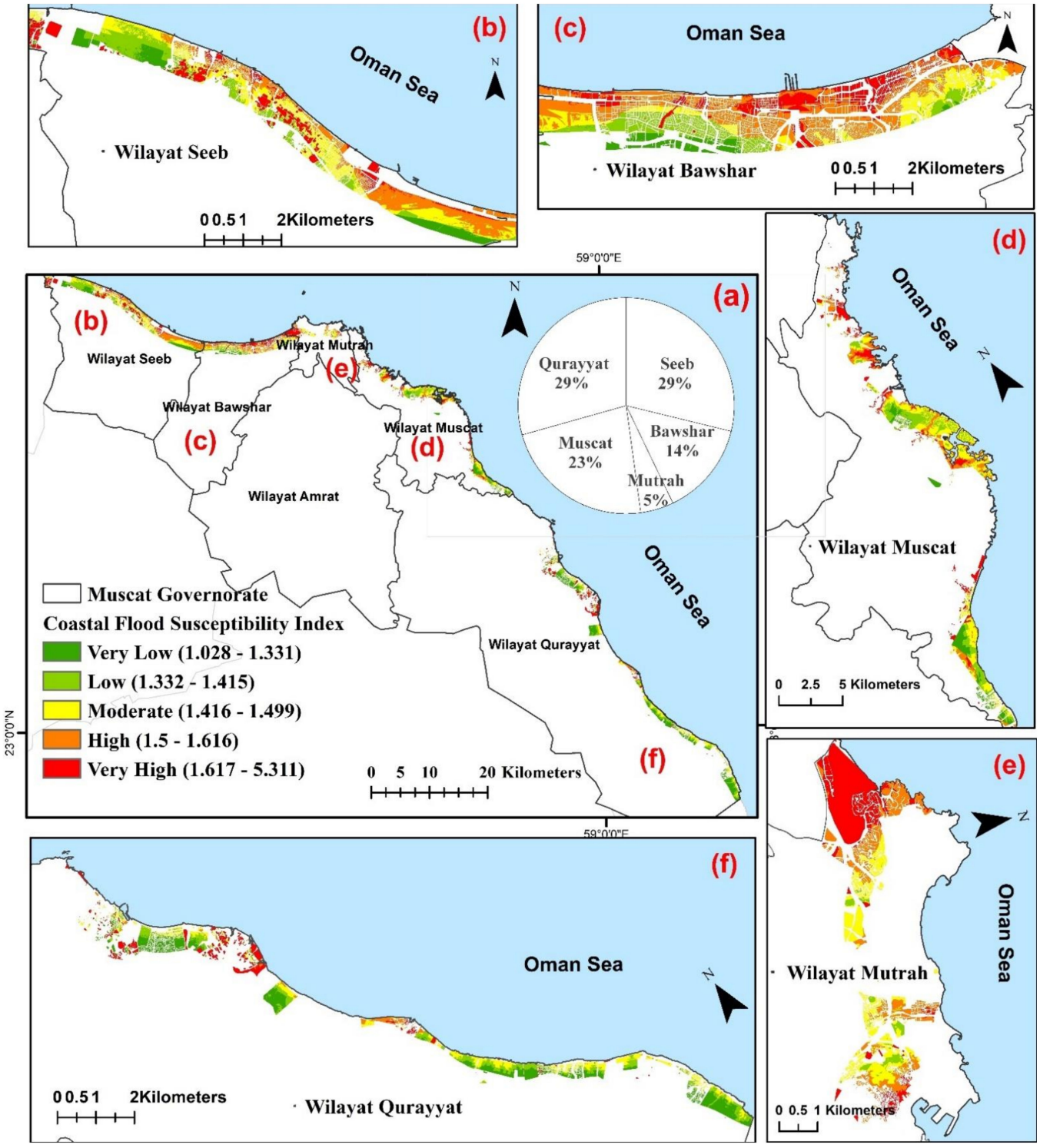

Figure 5. Coastal Flood Susceptibility Index for The (**a**) Governorate of Muscat, (**b**) Wilayat Seeb, (**c**) Wilayat Bawshar, (**d**) Wilayat Muscat, (**e**) Wilayat Mutrah and (**f**) Wilayat Qurayyat.

According to the coastal flood susceptibility index, approximately 133.5 km^2 of the extracted area is threatened to coastal floods. Of this, 23.29 km^2 (17%) is identified as being a very high flood susceptibility zone, and about 27.59 km^2 (21%) is identified as being high susceptibility. The moderately susceptible zone constitutes 31.49 km^2 (24%), while the low and very low susceptibility zones make up approximately 51.2 km^2 (38%) of the exposed area. Within Wilayats, Wilayat Qurayyat receives the largest portion of this threat, with about 39.21 km^2 (29%) of the total threatened area, followed by Wilayat Seeb with about 38.5 km^2 (29%). On the other hand, the results indicated that the Wilayats of Muscat, Bawshar, and Mutrah are threatened by floods with about 30.42 km^2 (23%), 18.79 km^2 (14%), and 6.62 km^2 (5%), respectively. The most common reasons for Wilayat Qurayyat receiving the largest portion of this hazard are the area of the Wilayat compared to other Wilayats, while the most common reasons for Wilayat Seeb receiving this hazard are the high rates of population and urbanization in the area. Furthermore, the type of land use and HSG factors also contribute greatly to flood risk in these Wilayats according to the entropy model.

5. Conclusions

The Governorate of Muscat has been frequently affected by floods and their related destruction. Therefore, assessing the likelihood of flooding and the extent of areas that are susceptible to this hazard has become an essential part of prediction and mitigation strategies. In this study, Shannon's entropy model was initially used to map and to predict the role of seven influencing factors in causing coastal floods. According to the obtained entropy results, land use and HSG factors have the greatest relationships with flood occurrence in the given area, as they play a major role in water infiltration and surface runoff. On the other hand, slope degree influencing factor has the lowest effect on flood susceptibility. In the next step, the coastal flood susceptibility index was calculated using Equation (5). Finally, the coastal flood susceptibility zonation map was produced by categorizing the flood susceptibility index using the quantile classification method into five flood potential classes including very high, high, moderate, low, and very low. As a result, 133.5 km^2 representing 36% of the extracted area is at risk of flooding.

Based on the overall assessment, the result of this study can serve as a useful reference material for future studies. Local government agencies and decision-makers can also adopt the susceptibility map produced in this study as a preliminarily step in overall flood management programs and strategies to mitigate potential flood damages and losses. As a further step, it is recommended to validate the accuracy of the obtained result by comparing it with a real flooding event, such as flooding during cyclones Gonu and Phet.

Author Contributions: Conceptualization, Hanan Al-Hinai and Rifaat Abdalla; methodology, Hanan Al-Hinai; software, Hanan Al-Hinai; formal analysis, Hanan Al-Hinai; investigation, Hanan Al-Hinai and Rifaat Abdalla; resources, Hanan Al-Hinai and Rifaat Abdalla; data curation, Hanan Al-Hinai; writing—original draft preparation, Hanan Al-Hinai; writing—review and editing, Hanan Al-Hinai and Rifaat Abdalla; supervision, Rifaat Abdalla. All authors have read and agreed to the published version of the manuscript.

Funding: This research received no external funding.

Data Availability Statement: The data presented in this study are not publicly available due to privacy restrictions.

Acknowledgments: The authors would like to express their appreciation and thank the Ministry of Agriculture, Fisheries and Water Resources, and the National Centre for Statistics and Information for providing the necessary data. The authors gratitude is also extended to the editor and anonymous reviewers for their efforts in reviewing the paper and their constructive suggestions and comments that have greatly aided in the improvement of the manuscript.

Conflicts of Interest: The authors declare no conflict of interest.

References

1. Climate Change Effects—Coasts—Environment—European Commission. Available online: https://ec.europa.eu/environment/iczm/state_coast.htm (accessed on 17 January 2021).
2. Samanta, R.K.; Bhunia, G.S.; Shit, P.K.; Pourghasemi, H.R. Flood Susceptibility Mapping Using Geospatial Frequency Ratio Technique: A Case Study of Subarnarekha River Basin, India. *Model. Earth Syst. Environ.* **2018**, *4*, 395–408. [CrossRef]
3. Cred Crunch Newsletter, Issue No. 58 (April 2020)—Disaster 2019: Year in Review. Available online: https://reliefweb.int/report/world/cred-crunch-newsletter-issue-no-58-april-2020-disaster-2019-year-review (accessed on 5 April 2021).
4. EM-DAT Glossary. Available online: https://www.emdat.be/Glossary#letter_c (accessed on 5 April 2021).
5. The Centers for Disease Control and Prevention (CDC). *Coastal Flooding, Climate Change, and Your Health: What You Can Do to Prepare*; The Centers for Disease Control and Prevention (CDC): Atlanta, GA, USA, 2017.
6. Tehrany, M.S.; Kumar, L.; Shabani, F. A Novel GIS-Based Ensemble Technique for Flood Susceptibility Mapping Using Evidential Belief Function and Support Vector Machine: Brisbane, Australia. *PeerJ* **2019**, *7*. [CrossRef]
7. Abdalla, R. *An Infrastructure Interdependency-Based Framework for Utilizing Network-Centric GIS as a Core Technology in Disaster Management*, 1st ed.; Scholars' Press: Mauritius, 2018; ISBN 978-620-2-31105-2.
8. Rahman, M.; Ningsheng, C.; Islam, M.M.; Dewan, A.; Iqbal, J.; Washakh, R.M.A.; Shufeng, T. Flood Susceptibility Assessment in Bangladesh Using Machine Learning and Multi-Criteria Decision Analysis. *Earth Syst. Environ.* **2019**, *3*, 585–601. [CrossRef]
9. Santangelo, N.; Santo, A.; Di Crescenzo, G.; Foscari, G.; Liuzza, V.; Sciarrotta, S.; Scorpio, V. Flood Susceptibility Assessment in a Highly Urbanized Alluvial Fan: The Case Study of Sala Consilina (Southern Italy). *Nat. Hazards Earth Syst. Sci.* **2011**, *11*, 2765–2780. [CrossRef]
10. El-Haddad, B.A.; Youssef, A.M.; Pourghasemi, H.R.; Pradhan, B.; El-Shater, A.-H.; El-Khashab, M.H. Flood Susceptibility Prediction Using Four Machine Learning Techniques and Comparison of Their Performance at Wadi Qena Basin, Egypt. *Nat. Hazards* **2020**, *105*, 83–114. [CrossRef]
11. Chowdhuri, I.; Pal, S.C.; Chakrabortty, R. Flood Susceptibility Mapping by Ensemble Evidential Belief Function and Binomial Logistic Regression Model on River Basin of Eastern India. *Adv. Space Res.* **2020**, *65*, 1466–1489. [CrossRef]
12. Tehrany, M.S.; Kumar, L.; Jebur, M.N.; Shabani, F. Evaluating the Application of the Statistical Index Method in Flood Susceptibility Mapping and Its Comparison with Frequency Ratio and Logistic Regression Methods. *Geomat. Nat. Hazards Risk* **2019**, *10*, 79–101. [CrossRef]
13. Tehrany, M.S.; Jones, S.; Shabani, F. Identifying the Essential Flood Conditioning Factors for Flood Prone Area Mapping Using Machine Learning Techniques. *Catena* **2019**, *175*, 174–192. [CrossRef]
14. Abu El-Magd, S.A.; Amer, R.A.; Embaby, A. Multi-Criteria Decision-Making for the Analysis of Flash Floods: A Case Study of Awlad Toq-Sherq, Southeast Sohag, Egypt. *J. Afr. Earth Sci.* **2020**, *162*, 103709. [CrossRef]
15. Khosravi, K.; Pham, B.T.; Chapi, K.; Shirzadi, A.; Shahabi, H.; Revhaug, I.; Prakash, I.; Tien Bui, D. A Comparative Assessment of Decision Trees Algorithms for Flash Flood Susceptibility Modeling at Haraz Watershed, Northern Iran. *Sci. Total Environ.* **2018**, *627*, 744–755. [CrossRef] [PubMed]
16. Al-Hinai, H.Y.; Abdalla, R. Spatial Prediction of Coastal Flood Susceptible Areas in Muscat Governorate Using an Entropy Weighted Method. In *WIT Transactions on Engineering Sciences*; WIT Press: Southampton, UK, 2020; Volume 129, pp. 121–133.
17. Liu, Y.B.; De Smedt, F. Flood Modeling for Complex Terrain Using GIS and Remote Sensed Information. *Water Resour. Manag.* **2005**, *19*, 605–624. [CrossRef]
18. Costache, R.; Pham, Q.B.; Avand, M.; Thuy Linh, N.T.; Vojtek, M.; Vojteková, J.; Lee, S.; Khoi, D.N.; Thao Nhi, P.T.; Dung, T.D. Novel Hybrid Models Between Bivariate Statistics, Artificial Neural Networks and Boosting Algorithms for Flood Susceptibility Assessment. *J. Environ. Manag.* **2020**, *265*, 110485. [CrossRef] [PubMed]
19. Charlton, R.; Fealy, R.; Moore, S.; Sweeney, J.; Murphy, C. Assessing the Impact of Climate Change on Water Supply and Flood Hazard in Ireland Using Statistical Downscaling and Hydrological Modelling Techniques. *Clim. Chang.* **2006**, *74*, 475–491. [CrossRef]
20. Liu, B. Modelling Multi-Hazard Risk Assessment: A Case Study in the Yangtze River Delta, China. Ph.D. Thesis, University of Leeds, Leeds, UK, 2015.
21. Liu, B.; Siu, Y.L.; Mitchell, G. Hazard Interaction Analysis for Multi-Hazard Risk Assessment: A Systematic Classification Based on Hazard-Forming Environment. *Nat. Hazards Earth Syst. Sci.* **2016**, *16*, 629–642. [CrossRef]
22. Costache, R.; Pham, Q.B.; Sharifi, E.; Linh, N.T.T.; Abba, S.I.; Vojtek, M.; Vojteková, J.; Nhi, P.T.T.; Khoi, D.N. Flash-Flood Susceptibility Assessment Using Multi-Criteria Decision Making and Machine Learning Supported by Remote Sensing and GIS Techniques. *Remote Sens.* **2020**, *12*, 106. [CrossRef]
23. Shannon, C.E. A Mathematical Theory of Communication. *Bell Syst. Tech. J.* **1948**, *27*, 379–423. [CrossRef]
24. Jaafari, A.; Najafi, A.; Pourghasemi, H.R.; Rezaeian, J.; Sattarian, A. GIS-Based Frequency Ratio and Index of Entropy Models For Landslide Susceptibility Assessment in the Caspian Forest, Northern Iran. *Int. J. Environ. Sci. Technol.* **2014**, *11*, 909–926. [CrossRef]
25. Liu, R.; Chen, Y.; Wu, J.; Gao, L.; Barrett, D.; Xu, T.; Li, X.; Li, L.; Huang, C.; Yu, J. Integrating Entropy-Based Naïve Bayes and GIS for Spatial Evaluation of Flood Hazard. *Risk Anal.* **2017**, *37*, 756–773. [CrossRef]
26. Haghizadeh, A.; Siahkamari, S.; Haghiabi, A.H.; Rahmati, O. Forecasting Flood-Prone Areas Using Shannon's Entropy Model. *J. Earth Syst. Sci.* **2017**, *126*, 39. [CrossRef]

27. Siahkamari, S.; Haghizadeh, A.; Zeinivand, H.; Tahmasebipour, N.; Rahmati, O. Spatial Prediction of Flood-Susceptible Areas Using Frequency Ratio and Maximum Entropy Models. *Geocarto Int.* **2018**, *33*, 927–941. [CrossRef]
28. Arora, A.; Pandey, M.; Siddiqui, M.A.; Hong, H.; Mishra, V.N. Spatial Flood Susceptibility Prediction in Middle Ganga Plain: Comparison of Frequency Ratio and Shannon's Entropy Models. *Geocarto Int.* **2019**, 1–32. [CrossRef]
29. Hereher, M.E. Estimation of Monthly Surface Air Temperatures from MODIS LST Time Series Data: Application to the Deserts in the Sultanate of Oman. *Environ. Monit. Assess.* **2019**, *191*, 592. [CrossRef] [PubMed]
30. Al-Awadhi, T. The use of RS and GIS to evaluate the effects of tropical cyclones: A case study from A'Seeb, Muscat after GONU cyclone. In *WWRP 2010-2, Proceedings of the 1st WMO International Conference on Indian Ocean Tropical Cyclones and Climate Change, Muscat, Sultanate of Oman, 8–11 March 2009*; World Meteorological Organization: Geneva, Switzerland, 2010; pp. 95–104.
31. Ministry of Interior Web Site, Sultanate of Oman. Available online: https://www.moi.gov.om/ar-om/governorates/muscat (accessed on 5 April 2021).
32. National Centre for Statistics and Information Population Dashboard. Available online: https://portal.ecensus.gov.om/ecen-portal/ (accessed on 16 January 2021).
33. Al-Awadhi, T.; Choudri, B.S.; Charabi, Y. Growth of Coastal Population: Likely Exposure to Sea Level Rise and Associated Storm Surge Flooding in the Sultanate of Oman. *J. Environ. Manag. Tour.* **2016**, *7*. [CrossRef]
34. Beuzen-Waller, T.; Stéphan, P.; Pavlopoulos, K.; Desruelles, S.; Marrast, A.; Puaud, S.; Giraud, J.; Fouache, É. Geoarchaeological Investigation of the Quriyat Coastal Plain (Oman). *Quat. Int.* **2019**, *532*, 98–115. [CrossRef]
35. Kwarteng, A.Y. Remote sensing imagery assessment of areas severely affected by cyclone Gonu in Muscat, Sultanate of Oman. In *Indian Ocean Tropical Cyclones and Climate Change*; Charabi, Y., Ed.; Springer: Dordrecht, The Netherlands, 2010; pp. 223–232. ISBN 978-90-481-3108-2.
36. Al-Rawas, G.A.; Valeo, C.; Khan, U.T.; Al-Hafeedh, O.H. Effects of Urban Form on Wadi Flow Frequency Analysis in the Wadi Aday Watershed in Muscat, Oman. *Urban Water J.* **2015**, *12*, 263–274. [CrossRef]
37. Al-Rawas, G.A. Flash Flood Modelling in Oman Wadis. Ph.D. Thesis, Department of Civil Engineering, University of Calgary, Calgary, AB, Canada, 2009.
38. Al-Hinai, H.Y. Tsunami Risk Assessment along the Coast of the Sultanate of Oman Using Geospatial Technologies. Master's Thesis, Arabian Gulf University, Manama, Bahrain, 2013.
39. Al-Hatrushi, S.; Al-Alawi, H. Evaluating the impact of flood hazard caused by tropical cyclones on land use using remote sensing and GIS in Wadi Uday: Sultanate of Oman. In Proceedings of the 34th International Symposium on Remote Sensing of Environment-The GEOSS Era: Towards Operational Environmental Monitoring, Sidney, NSW, Australia, 10–15 April 2011.
40. Byrne, D.E.; Sykes, L.R.; Davis, D.M. Great Thrust Earthquakes and Aseismic Slip along the Plate Boundary of the Makran Subduction Zone. *J. Geophys. Res. Solid Earth* **1992**, *97*, 449–478. [CrossRef]
41. Okal, E.A.; Fritz, H.M.; Raad, P.E.; Synolakis, C.; Al-Shijbi, Y.; Al-Saifi, M. Oman Field Survey after the December 2004 Indian Ocean Tsunami. *Earthq. Spectra* **2006**, *22*, 203–218. [CrossRef]
42. Tehrany, M.S.; Kumar, L. The Application of a Dempster–Shafer-Based Evidential Belief Function in Flood Susceptibility Mapping and Comparison with Frequency Ratio and Logistic Regression Methods. *Environ. Earth Sci.* **2018**, *77*, 1–24. [CrossRef]
43. Rahmati, O.; Zeinivand, H.; Besharat, M. Flood Hazard Zoning in Yasooj Region, Iran, Using GIS and Multi-Criteria Decision Analysis. *Geomat. Nat. Hazards Risk* **2016**, *7*, 1000–1017. [CrossRef]
44. Khosravi, K.; Nohani, E.; Maroufinia, E.; Pourghasemi, H.R. A GIS-Based Flood Susceptibility Assessment and Its Mapping in Iran: A Comparison Between Frequency Ratio and Weights-of-Evidence Bivariate Statistical Models with Multi-Criteria Decision-Making Technique. *Nat. Hazards* **2016**, *83*, 947–987. [CrossRef]
45. Ibrahim-Bathis, K.; Ahmed, S.A. Geospatial Technology for Delineating Groundwater Potential Zones in Doddahalla Watershed of Chitradurga District, India. *Egypt. J. Remote Sens. Space Sci.* **2016**, *19*, 223–234. [CrossRef]
46. Nielsen, R.D.; Hjelmfelt, A.T. Hydrologic Soil Group Assignment. *Proc. Water Resour. Eng.* **1998**, 1297–1302.
47. Rahmati, O.; Pourghasemi, H.R.; Zeinivand, H. Flood Susceptibility Mapping Using Frequency Ratio and Weights-of-Evidence Models in the Golastan Province, Iran. *Geocarto Int.* **2016**, *31*, 42–70. [CrossRef]
48. Al-Zahrani, M.; Al-Areeq, A.; Sharif, H.O. Estimating Urban Flooding Potential Near the Outlet of an Arid Catchment in Saudi Arabia. *Geomat. Nat. Hazards Risk* **2017**, *8*, 672–688. [CrossRef]
49. Shuster, W.; Bonta, J.; Thurston, H.; Warnemuende, E.; Smith, D.R. Impacts of Impervious Surface on Watershed Hydrology: A Review. *Urban Water J.* **2005**, *2*, 263–275. [CrossRef]
50. National Center for Statistics and Information Oman. National Spatial Data Infrastructure (NSDI). Available online: https://ncsi.gov.om/Pages/NCSI.aspx (accessed on 5 April 2021).
51. Tehrany, M.S.; Pradhan, B.; Mansor, S.; Ahmad, N. Flood Susceptibility Assessment Using GIS-Based Support Vector Machine Model with Different Kernel Types. *Catena* **2015**, *125*, 91–101. [CrossRef]
52. Data Classification Methods—ArcGIS Pro. Documentation. Available online: https://pro.arcgis.com/en/pro-app/help/mapping/layer-properties/data-classification-methods.htm (accessed on 27 April 2020).
53. Chapi, K.; Singh, V.P.; Shirzadi, A.; Shahabi, H.; Bui, D.T.; Pham, B.T.; Khosravi, K. A Novel Hybrid Artificial Intelligence Approach for Flood Susceptibility Assessment. *Environ. Model. Softw.* **2017**, *95*, 229–245. [CrossRef]
54. Jawarneh, R.N.; Almushaiki, S.S. Role of Physical Settings on Increasing Flood Hazard in Muscat Built-up Areas (2007–2015) Using GIS. *J. Arts Soc. Sci.* **2018**, *9*, 65–78. [CrossRef]